Magazine of Civil Engineering. 2019. 89(5). Pp. 106–114
Инженерно-строительный журнал. 2019. № 5(89). С. 106–114

Magazine of Civil Engineering

ISSN 2071-0305

journal homepage: http://engstroy.spbstu.ru/

DOI: 10.18720/MCE.89.9

Water permeation simulation of autoclaved aerated concrete blocks using the Lattice Boltzmann method

F. Jun*, Y. Yue, Y. JiaBin
School of Civil Engineering and Architecture, Zhejiang Sci-Tech University, Hangzhou, China
** E-mail: fujun@zstu.edu.cn*

Keywords: autoclaved aerated concrete block, LBM, penetration, flow simulation, MATLAB

Abstract. In this paper, the Lattice Boltzmann Method (LBM) is used to simulate the seepage field of autoclaved aerated concrete blocks. The macroscopic permeability coefficients of aerated blocks are obtained. The complex flow characteristics of the internal flow field are revealed. A stochastic four-parameter growth method (QSGS) based on the distribution probability of initial growth nuclei and porosity is proposed. A meso-model of the real pore structure of aerated blocks is established. The influence of initial inlet pressure and model porosity on the permeability of aerated block is analyzed by numerical calculation of the permeability development process of aerated block. The results show that the two-dimensional meso-model close to the real pore structure of aerated block can be constructed by the stochastic four-parameter growth method; the water permeability coefficient of aerated block calculated by the LBM numerical method is in good agreement with the experimental results; under certain conditions, the linear relationship between the permeability coefficient of autoclaved aerated concrete block and its porosity satisfies the requirement of practical engineering application. It has certain guiding significance for practical engineering application.

1. Introduction

Autoclaved aerated concrete blocks are some of the most widely used new wall materials. They have a porosity of 65–80 % and the advantages of being light weight, fire resistant, heat preserving and convenient in terms of construction [1–3]. However, in bad weather conditions, rainwater easily enters the interior of the wall from the pore isotonic passage, which causes a decline in thermal insulation performance and durability of the wall. Thus, the leakage of the wall cannot be ignored [4]. Currently, few studies have been conducted on the permeability of autoclaved aerated concrete blocks and on seepage simulation methods at the mesoscopic level. Because micro-factors such as pore structure and pore distribution of aerated blocks can reflect the macro-properties of aerated blocks and affect their macro-permeability, studying the permeability of autoclaved aerated concrete blocks at the micro-level is of great theoretical value [5–6].

As a highly efficient fluid dynamics simulation method, the lattice Boltzmann method (LBM) is widely used in the field of porous media seepage because of its powerful boundary processing and excellent parallel computing capabilities. Hazlett [7] simulated a multiphase flow inside the pores of porous media successfully based on the LBM. Degruyter et al. Reconstructed volcanic pumice using synchronous accelerated computed tomography (CT) imaging technology while studying the relationship between the porosity and permeability of volcanic pumice using the LBM method [8]. Qian [9] used a single relaxation incompressible LBM model to simulate a flow field in a two-dimensional porous media model at the mesoscopic level, which verified the accuracy of Darcy's law, and proposed an efficient and simple permeability calculation method. Luo [10] used the LBM to simulate fluid flow in random porous media and tested Darcy's law. Li [11] constructed a porous media model based on the quartet structure generation set (QSGS) and then calculated the permeability of porous media using an LBM program compiled by MATLAB software.

Jun, F., Yue, Y., JiaBin, Y. Water Permeation Simulation of Autoclaved Aerated Concrete Blocks using the Lattice Boltzmann Method. Magazine of Civil Engineering. 2019. 89(5). Pp. 106–114. DOI: 10.18720/MCE.89.9

Джун Ф., Юэ Ф., Джиабин Й. Моделирование водопроницаемости газобетонных блоков методом решёточных уравнений Больцмана // Инженерно-строительный журнал. 2019. № 5(89). С. 106–104. DOI: 10.18720/MCE.89.9

The key to successfully simulating the water infiltration process of autoclaved aerated concrete blocks is to describe quantitatively the pore structure characteristics using appropriate methods [1–4]. In 2007, the QSGS proposed by Wang et al. [15] was shown to solve the aforementioned problems effectively. The solid phase growth process effectively considers the solid particle size, random distribution of the solid phase, and statistical properties of the model. When the parameters are adjusted, a mesoscopic model closer to a real aerated block can be obtained, and the reconstructed mesoscopic model of an aerated block can be combined with the LBM to make the calculation more efficient.

A QSGS combined with the LBM can simulate the water infiltration process effectively in autoclaved aerated concrete blocks. Therefore, a simple and efficient QSGS is proposed in this study. Then, based on the LBM, the infiltration process in the two-dimensional micro-model of the aerated block is accurately revealed by numerical calculation, and the influence of the initial inlet pressure and model porosity on the permeability coefficient of the model is analyzed. The linear relationship between the permeability coefficient and porosity of autoclaved aerated concrete blocks is finally established.

2. Methods

2.1. Lattice Boltzmann method model

The macroscopic motion of fluid can be simulated by solving the Boltzmann equation numerically. The Boltzmann equation can be expressed as

$$\frac{\partial f}{\partial t} + c \cdot \nabla f = -\frac{1}{\tau}[f - f^{\text{eq}}], \tag{1}$$

where $f = f(r, c, t)$ represents the number of molecules in the unit volume at a speed of $c \sim c + dc$ at a time of t and position of r;

τ denotes the relaxation factor;

f^{eq} represents the equilibrium distribution function.

The most representative two-dimensional square lattice D2Q9 model in LBM is applied. According to the discrete velocity distribution of mesh and fluid particles, each fluid particle has nine moving directions (including the static state of particles). The corresponding velocity in each direction can be expressed as [16]

$$e_i = \begin{cases} (0,0) & \ldots\ i = 0, \\ c\left(\cos\left[(i-1)\frac{\pi}{2}\right], \sin\left[(i-1)\frac{\pi}{2}\right]\right) & \ldots\ i = 1, 2, 3, 4, \\ \sqrt{2}c\left(\cos\left[(2i-1)\frac{\pi}{4}\right], \sin\left[(2i-1)\frac{\pi}{4}\right]\right) & \ldots\ i = 5, 6, 7, 8, \end{cases} \tag{2}$$

where c represents the lattice velocity with $c = \delta_x / \delta_t$, δ_x represents the grid step size, and δ_t represents the time step. Then (1) can be discretized into

$$f_i(\boldsymbol{x} + \boldsymbol{e_i}\Delta t, t + \Delta t) - f_i(\boldsymbol{x}, t) = -\frac{1}{\tau}[f_i(\boldsymbol{x}, t) - f_i^{\text{eq}}(\boldsymbol{x}, t)]. \tag{3}$$

The equilibrium distribution function is expressed as [16]

$$f_i^{\boldsymbol{eq}} = \omega_i \rho[1 + \frac{3}{c_s^2}(\boldsymbol{e_i} \cdot \boldsymbol{u}) + \frac{9}{2c_s^4}(\boldsymbol{e_i} \cdot \boldsymbol{u})^2 - \frac{3}{2c_s^2}u^2] \tag{4}$$

where ρ represents the macroscopic density of fluid;

u represents the macroscopic velocity;

$c_s = \frac{c}{\sqrt{3}}$ represents the base lattice velocity;

ω_i represents the weight coefficient.

$$\omega_i = \begin{cases} 4/9 & \ldots\ i = 0, \\ 1/9 & \ldots\ i = 1, 2, 3, 4, \\ 1/36 & \ldots\ i = 5, 6, 7, 8. \end{cases} \tag{5}$$

According to the law of conservation of mass and momentum, the macro-density of fluid can be expressed by the sum of distribution functions in each grid node, and the macro-velocity of fluid can be expressed by the product of the micro-velocity per unit mass and distribution function in the direction of the lattice, which can be represented as $\rho \boldsymbol{u}$. Therefore, the distribution function of particles satisfies the following equation [17]:

$$\rho = \sum_i f_i, \qquad \rho \boldsymbol{u} = \sum_i f_i \boldsymbol{e}_i. \tag{6}$$

By the Chapman–Enskog expansion [18] of the evolution equation, the macroscopic Navier–Stokes equation corresponding to the single relaxation model can then be obtained:

$$\partial_t \rho + \nabla \cdot (\rho \boldsymbol{u}) = 0; \tag{7}$$

$$\partial_t (\rho \boldsymbol{u}) + \nabla \cdot (\rho \boldsymbol{u}\boldsymbol{u}) = -\nabla p + \nabla \cdot \left[\rho \upsilon (\nabla \boldsymbol{u} + (\nabla \boldsymbol{u})^T) \right], \tag{8}$$

where $p = \rho c_s^2$ and $\upsilon = c_s^2 \left(\tau - \frac{1}{2} \right) \Delta t$ represents kinematic viscosity.

2.2. Boundary condition

The seepage process of water in an aeration block is limited by the solid wall. When the LBM is used to simulate the seepage process of the aeration block, appropriate boundary conditions must be selected to deal with all points on the wall. The standard rebound and periodic boundary treatment schemes are adopted in this study. For the collision between solid skeleton and fluid particles, the rebound treatment which is called the standard rebound scheme in LBM, is typically used (Figure 1).

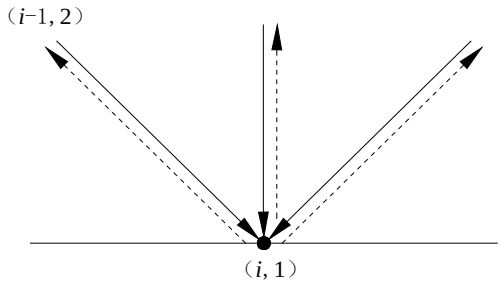

Figure 1. Label bounce format.

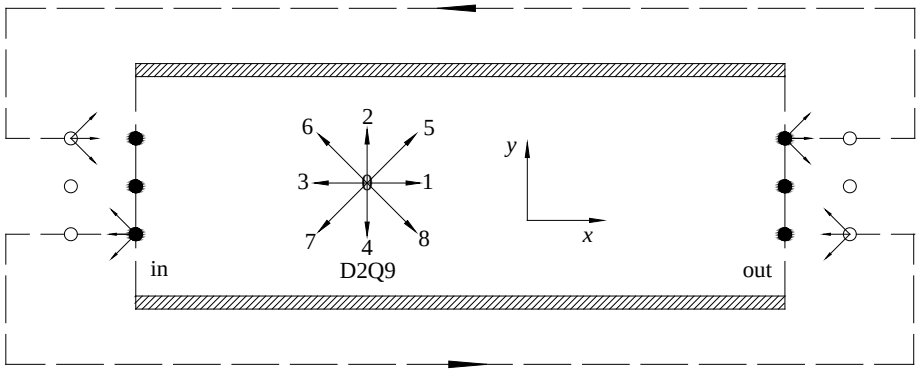

Figure 2. Periodic boundary format.

If the flow field is periodic in space or infinite in one direction, the periodic boundary treatment scheme [19] can be used at the corresponding boundary. A schematic diagram of the periodic boundary treatment scheme (Figure 2) shows that solid and hollow circles represent fluid and virtual fluid nodes, respectively. The periodic boundary processing format can be expressed as

$$\begin{cases} f_{1,5,8}(0, j) = f_{1,5,8}(N_x, j), \\ f_{3,6,7}(N_x + 1, j) = f_{3,6,7}(1, j), \end{cases} \tag{9}$$

where $f_{1,5,8}(0, j)$ and $f_{3,6,7}(N_x{+}1, j)$ represent distribution functions on the $(0, j)$ and $(N_x{+}1, j)$ nodes, respectively;

$f_{1,5,8}(N_x, j)$ and $f_{3,6,7}(1, j)$ represent distribution functions on the (N_x, j) and $(1, j)$ nodes, respectively.

2.3. Calculation of permeability coefficient

When fluid flows inside a porous medium, both the flow rate and Reynolds number are low (*Re*<10). The permeability of the porous medium can be obtained by Darcy's theorem, which can be expressed as [20]

$$\overline{u} = \frac{k}{\mu} \cdot \frac{\Delta P}{L}, \tag{10}$$

where $\overline{u}$ denotes the average velocity;

μ is the kinematic viscosity coefficient of fluid;

k represents permeability;

L denotes the permeation path of fluid in porous media;

ΔP is the pressure loss value of flow.

With the introduction of $K = \frac{k\rho g}{\mu}$, the permeability coefficient of the porous medium at a low flow rate can be obtained as follows:

$$K = \frac{\overline{u}\rho g L}{\Delta P}. \tag{11}$$

3. Results and Discussion

3.1. Construction of two-dimensional meso-model of an aeration block

The development route of water infiltration in a block is not a straight line, but rather constitutes multiple lines and directions. It is assumed that the fluid can flow only in the effective pore, and the distribution of the effective pore is interlaced and does not overlap along the height direction of the aeration block. In other words, the pore corresponding to the upper pore is randomly distributed in the next section.

An autoclaved aerated concrete block has many irregular pore distributions with different shapes. The length direction of the autoclaved aerated concrete block wall has a fatal research value as compared to the width direction. Therefore, a stochastic four-parameter growth method was used in this study to reconstruct a two-dimensional mesoscopic equivalent model of an aerated block by adjusting the initial growth core distribution probability and porosity. The solid phase of the aerated block is the growth phase, the pore phase is the non-growth phase, and the initial phase in the model area is the pore. Several growth phases are randomly distributed within the scope of the model, and they then grow in all directions with a set probability. The growth stops when the porosity of the model reaches the set porosity. The concrete reconstruction steps are described as follows:

1. In the model range, the solid phase growth nuclei are randomly arranged with probability P_{cd}, which is less than the volume fraction (porosity *n*) of the growth phase;

2. Each growth nucleus grows to its adjacent point with a preset probability P_i, and its growth direction is i, i = 1, 2, 3, …, 8, as shown in Figure 3;

3. Repeat Step 2 until the growth phase reaches its preset volume fraction (porosity *n*);

4. The growth nucleus stops growing and the porous medium is reconstructed.

The stochastic four-parameter growth method is a traditional and widely used method for constructing porous media. However, under the premise of known permeability coefficient of porous media, few studies on the application of the equivalent model for constructing porous media by adjusting parameters have been reported. In this study, the sizes of solid particles, the random distribution of solid phases, and the statistical characteristics of the model were all controlled by adjusting the four parameters of initial growth probability (P_{cd}), growth probability in all directions (P_i), growth probability in the i direction ($P^{(nm)}$), and model porosity (*n*).The reconstructed aerated block mesoscopic model more closely resembles a real aerated block, and a prerequisite is provided for studying the impermeability of the aerated block and its internal water infiltration process.

3.2. Simulation calculation and analysis

3.2.1. Determining simulation parameters

The mesh size selected in this simulation was 100×100, the porosity of the model was n = 70 %, R_{e} = 10, and the micro-model of the aeration block is shown in Figure 4. The upper and lower boundaries of the model were established as impermeable boundaries, and the standard rebound scheme was applied. The left and right boundaries were established as the entrance and exit of the flow field, respectively, and the periodic boundary was adopted. The pore and solid boundary adopted the standard rebound scheme. Water flowed into the model from the inlet at different pressures and flowed from left to right as driven by the pressure differential.

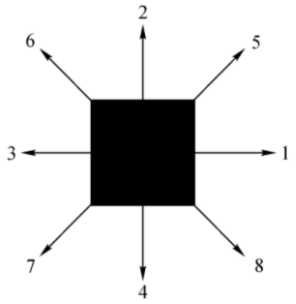

Figure 3. Growth direction of the two-dimensional QSGS growth phase.

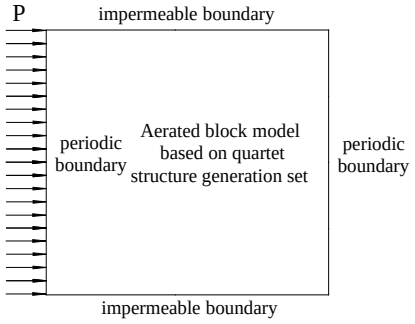

Figure 4. Aerated block penetration model.

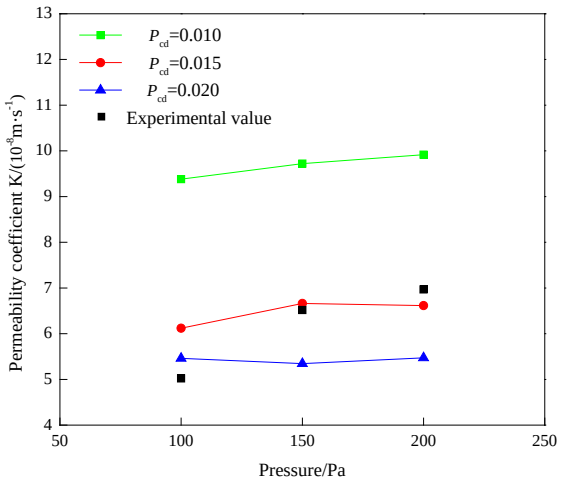

Figure 5. Permeability coefficient measured by an LBM simulation and experiment.

Figure 5 shows a comparison of the permeability coefficient of the A3.5 and B06 autoclaved aerated concrete blocks (n = 70 %) measured using the Darcy method with an LBM simulation value. It should be pointed out that the simulated values of permeability coefficients are discrete to some extent. Because the aeration block model must be reconstructed prior to each permeability simulation, a difference of pore volume, quantity, and connectivity in the different models is the results and thus a discretization of simulated values of permeability coefficients appears. Figure 5 shows that when the inlet water pressure was 150 Pa and the mesh size was 100×100, the average permeability coefficient of the two-dimensional mesoscopic model reconstructed by P_{cd} = 0.015 was K = 6.662×10^{-8} m/s, whereas the permeability coefficient of the aerator block obtained by the experiment under 150 Pa water pressure was K = 6.517×10^{-8} m/s. Figure 5 clearly shows that our numerical simulation results match those of the previous real test [21] very well, where the error range was within 2.2 %. Therefore, our numerical accuracy is reliable. The results show that when the inlet water pressure was 150 Pa and mesh size was 100×100, the two-dimensional mesoscopic model reconstructed by P_{cd} = 0.015 proved reliable for studying the water infiltration process and law at work inside the aerator block.

3.2.2. Relationship between the size of solid particles and permeability coefficient of the model

An autoclaved aerated concrete block is a kind of porous silicate masonry material made by internal gas generation. Therefore, the volume of its internal solid aggregate is different [22]. Large solid particles have smaller specific surface areas, but their pore size is usually greater than those of small solid particles. To study the effect of solid particle size on the permeability coefficient of aerator, different initial growth nucleus distribution probabilities were selected to reconstruct aerator models with different solid particle sizes and to simulate permeability.

Taking the porosity n = 70 % as an example, a two-dimensional micro-model of aerated blocks grown isotropically with initial growth nucleus distribution probabilities of P_{cd} = 0.01, 0.015 and 0.02 is presented in Figure 6.

Figures 6 and 7 clearly show that with a decrease in the initial growth nucleus distribution probability, the volume of solid particles increases, the connectivity of the model improves, and the permeability coefficient increases.

3.2.3. Relationship between porosity of aerated block and its permeability coefficient

As a porous material, the macroscopic permeability of an autoclaved aerated concrete block is usually related to its porosity [23–24]. However, due to the limitation of the test period and engineering environment, a direct test method is not suitable for a field test of the permeability coefficient of an aerated block.

Accordingly, this study examined the relationship between the porosity and permeability coefficient of an aerated block to characterize the permeability coefficient by porosity of the aerated block and in turn reflect its permeability resistance.

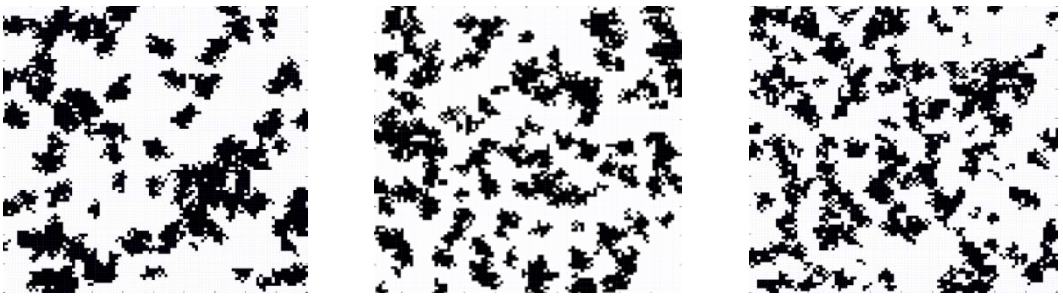

P_{cd} = 0.01 P_{cd} = 0.015 P_{cd} = 0.02

Figure 6. Reconstructed two-dimensional mesoscopic model.

Based on an LBM numerical calculation, the relationship between the porosity and permeability coefficient of an autoclaved aerated concrete block in a two-dimensional mesoscopic model was established in this study. Figure 8 shows the relationship between the porosity and permeability of a two-dimensional mesoscopic model of an autoclaved aerated concrete block. Figure 8 shows that the permeability coefficient of the model increases with an increase in its porosity. The relationship between the porosity and permeability coefficient of the model is linear and can be expressed as follows

$$K = 67.65n - 41.04, \quad (12)$$

where K represents the water permeability coefficient of the autoclaved aerated concrete block (unit: 10^{-8} m/s) and n represents its porosity.

Because the porosity of autoclaved aerated concrete blocks is generally in the range of 65–80 %, and the model porosity is also in this range when conducting a permeability simulation, the linear relationship between the porosity and permeability coefficient of aerated blocks is satisfied only when the porosity is in the range of 65–80 %.

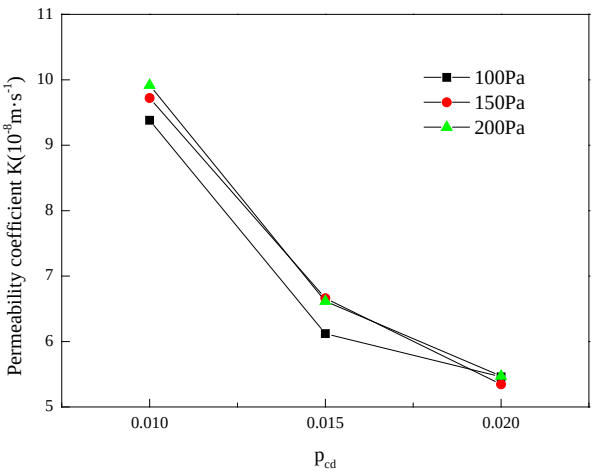

Figure 7. Relationship between solid particle size and model permeability coefficient.

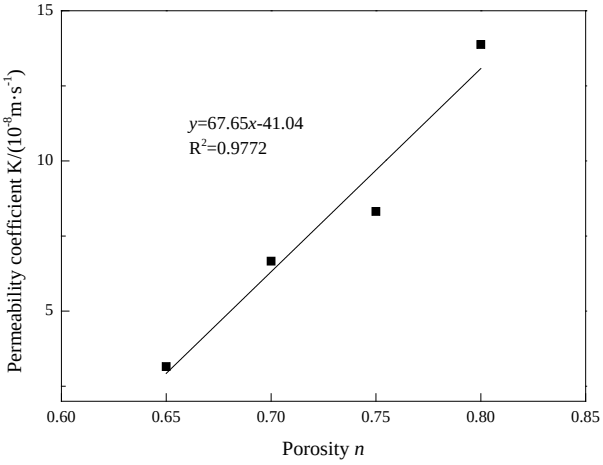

Figure 8. Relationship between porosity and permeability coefficient of the aerated block.

3.3. Analysis of water permeation process

To study further the water infiltration internal flow characteristics of the real pore structure of the aerated block, the water infiltration process of the two-dimensional mesoscopic model with porosities of 65, 70, and 75 % was calculated by LBM numerical values.

Figures 9–14 are the velocity vector and velocity distribution vectographs of the reconstructed two-dimensional mesoscopic model under a constant inlet water pressure (P = 150 Pa) with a mesh size of 100×100. These figures below show that at the initial stage of the pressure flow into the model (1000 δ_t), the flow velocity is distributed, but the flow direction basically follows the rule of «large pore inflow area». When the seepage is stable, the distribution of the flow velocity tends to be stable and, in the whole model, presents an obvious law, that is, the flow velocity in the through channel is greater. Simultaneously, several stable seepage channels are formed, namely, the “dominant channels” of seepage, and these «dominant channels» are mainly located in areas with good connectivity. In practical engineering, these «dominant passages» may be the easily seepage points on the wall. Therefore, studying the formation law and location of these passages to judge the seepage law of the wall and conducting the work of leakage prevention and repair of the wall have obvious engineering significance.

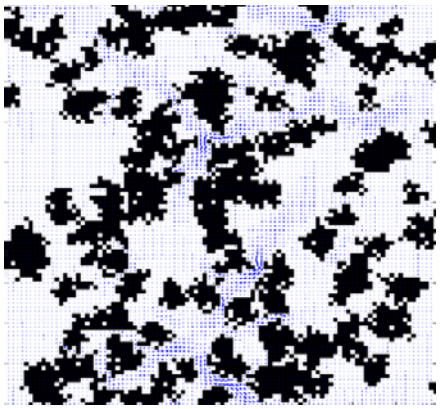

(a) Velocity vectograph at 1000δ_t

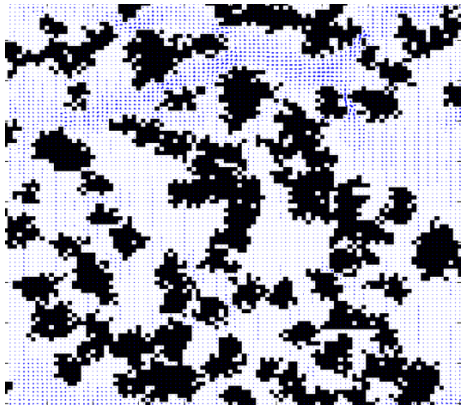

(b) Velocity vectograph of steady flow

Figure 9. Velocity vectograph in aerated block (n = 65 %).

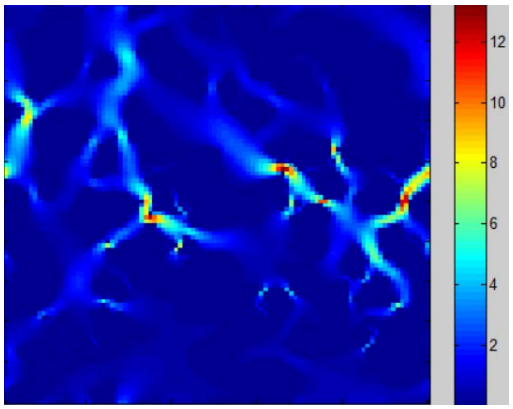

(a) Velocity distribution at 1000δ_t

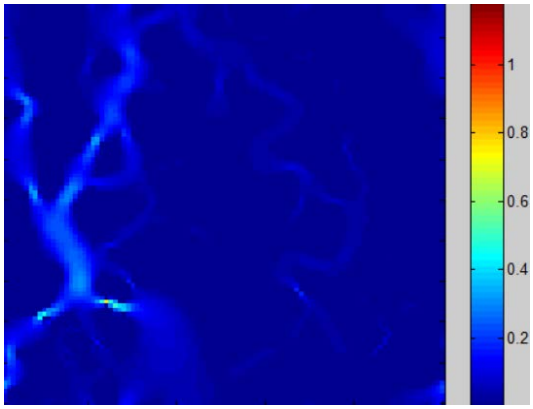

(b) Velocity distribution of steady flow

Figure 10. Velocity distribution in aerated block (n = 65 %).

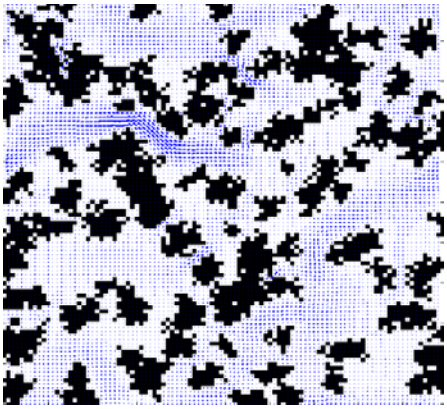

(a) Velocity vectograph at 1000δ_t

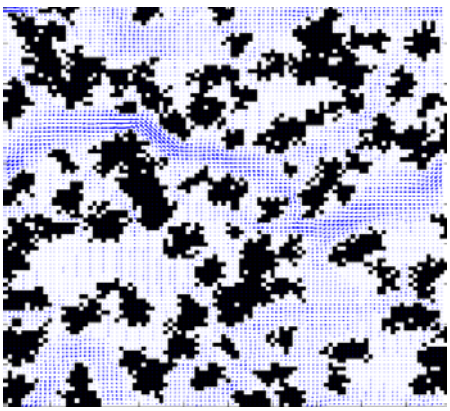

(b) Velocity vectograph of steady flow

Figure 11. Velocity vectograph in aerated block (n = 70 %).

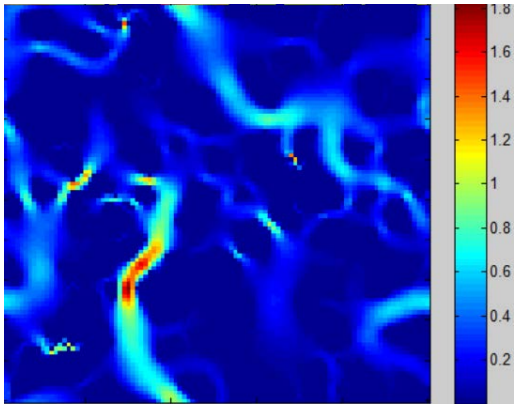

(a) Velocity distribution at 1000δ_t

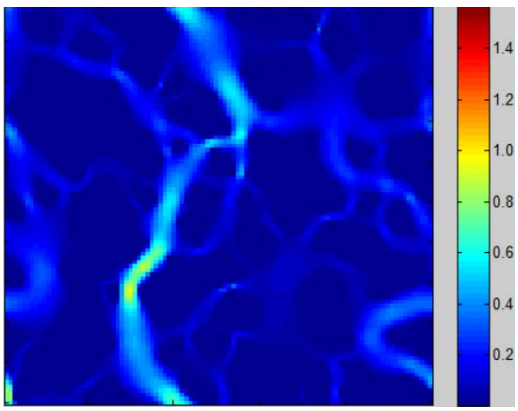

(b) Velocity distribution of steady flow

Figure 12. Velocity distribution in aerated block (n = 70 %)

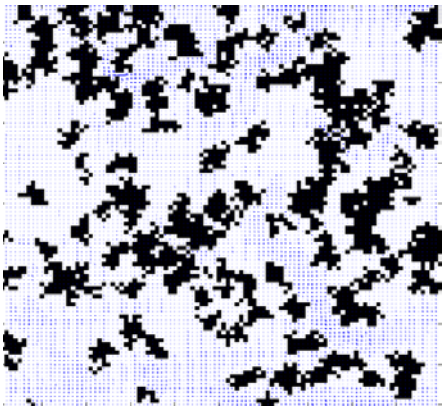

(a) Velocity vectograph at 1000δ_t

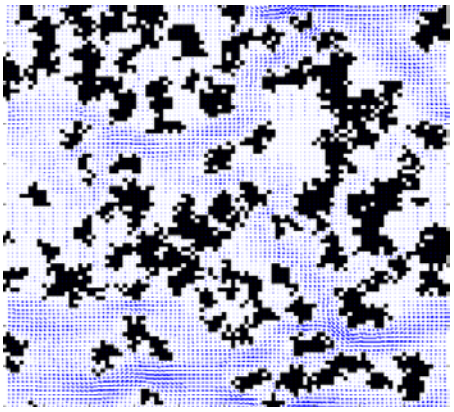

(b) Velocity vectograph of steady flow

Figure 13. Velocity vectograph in aerated block (*n* = 75 %).

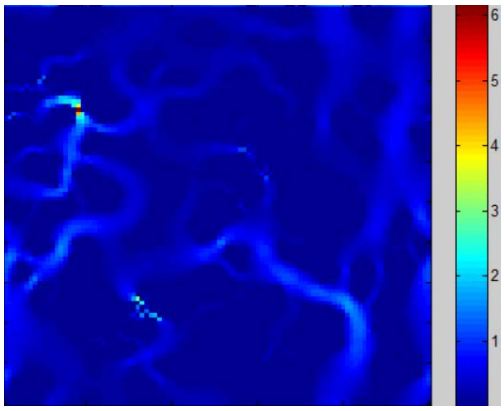

(a) Velocity distribution at 1000δ_t

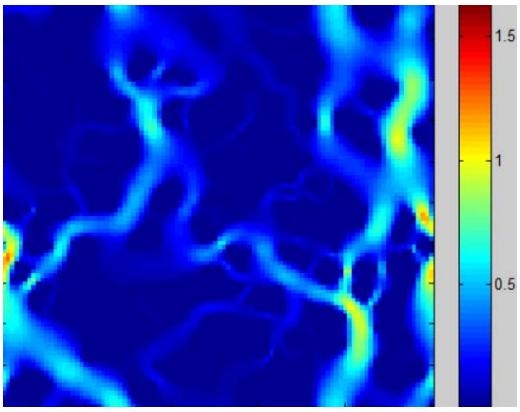

(b) Velocity distribution of steady flow

Figure 14. Velocity distribution in aerated block (*n* = 75 %).

4. Conclusion

Based on the LBM, a stochastic porous medium model was used to simulate the water infiltration process inside an autoclaved aerated concrete block. The following are the conclusions derived from this study:

1. When the micro-model of an autoclaved aerated concrete block was reconstructed by the QSGS, the pore structure of the model could be controlled by adjusting the porosity and initial growth nucleus distribution probability, and a two-dimensional micro-model resembling a real aerated block could be established.

2. When the inlet water pressure was 150 Pa and mesh size was 100×100, the permeability coefficient of the reconstructed two-dimensional mesoscopic model resembled that of the autoclaved aerated concrete block obtained from the experiment.

3. When the porosity of the two-dimensional mesoscopic model was in the range of 65–80 %, its permeability coefficient increased with increased porosity and effectively satisfied the linear relationship.

4. The water infiltration process inside the aerator block was shown to have an effective relationship with its pore connectivity. The water flow mainly flowed to the well-connected pore channel, and the flow velocity was greater in the through channel.

5. Acknowledgements

The authors would like to thank the Zhejiang Basic Public Welfare Research Project (LGF8E080016) and China Association for Engineering Construction Standardization for supporting this research project.

References

1. Jerman, M., Keppert, M., Vyborny, J., Cerny, R. Hygric, thermal and durability properties of autoclaved aerated concrete. Construction and Building Materials. 2013. Vol. 41. Pp. 352–359.
2. Schoendube, T., Rashid, S., Carrigan, S., Schoch, T., Kornadt, O. Autoclaved aerated concrete: Influence of heat storage capacity on thermal performance and thermal comfort. Mauerwerk. 2018. 22(5). Pp. 297–304.
3. Pukhkal, V.A., Mottaeva, A.B. FEM modeling of external walls made of autoclaved aerated concrete blocks. Magazine of Civil Engineering. 2018. 81(5). Pp. 203–212.

4. Pilon, B.S., Tyner, J.S., Yoder, D.C., Buchanan, J.R. The effect of pervious concrete on water quality parameters: a case study. Water. 2019. 11(2).
5. Fu, J., Zhou, Q.S., Ye, J.B. Summary of test methods for wall impermeability and d design of test equipment. Wall Materials Innovation & Energy Saving in Buildings. 2017. No. 12. Pp. 30–34. (Chinese).
6. Wang, H., Su, Y., Zhao Z., Wang W., Sheng G., Zhan S. Apparent permeability model for shale oil transport through elliptic nanopores considering wall-oil interaction. Journal of Petroleum Science and Engineering. 2019. Vol. 176. Pp. 1041–1052.
7. Hazlettr. Simulation of capillary-dominated displacements in microtomo graphic images of reservoir rocks. TransPorousMedia. 1995. No. 20. Pp. 21–35.
8. Degruyter, W., Burgisser, A., Bachmann, O., Malaspinas, O. Synchrotron X-ray microtomography and lattice Boltzmann simulations of gas flow through volcanic pumices. Geosphere. 2010. 6(6). Pp. 470–481.
9. Qian, J.Y., Li, Q., Xuan, Y.M., Yu, K. Application of Lattice-Boltzmann Scheme on Determining Flow Parameters of Porous Media. Journal of Engineering Thermophysics. 2004. 25(4). Pp. 655–657. (Chinese).
10. Luo, Z.X., Qiu, Y.J., Yu, H.Q. Computational Modeling of Flows in Random Porous Media using Lattice Boltzmann Method. Journal of Southwest Jiaotong University. 2014. 49(1). Pp. 93–96. (Chinese).
11. Li, J.Z., Zhao, Z.G., Tan, Y.L., Yang, Z.L., Song, L.L. Method of LBM for Isotropy Porous Medium of Permeability Calculation. Coal Technology. 2015. 34(8). Pp. 138–140. (Chinese).
12. Cui, G.Z., Shen, L.F., Wang, Z.L. Numerical simulation of mesoscopic seepage field of soil CT scanned slice based on lattice Boltzmann method. Rock and Soil Mechanics. 2016. 37(5). Pp. 1497–1502.
13. Shen, L.F., Wang, Z.L., Li, S.J. Numerical simulation for mesoscopic seepage field of soil based on lattice Boltzmann method at Rev scale. Rock and Soil Mechanics. 2015. 36. Pp. 689–694.
14. Fan, H., Zheng, H. MRT-LBM-based numerical simulation of seepage flow through fractal fracture networks. Science China-Technological Sciences. 2013. 56(12). Pp. 3115–3122.
15. Wang, M., Pan, N. Numerical analyses of effective dielectric constant of multiphase micro-porous media. Journal of Applied Physics. 2007. 101(11). Pp. 114102-1–114120-8.
16. Qian, Y.H., Humieres, D.D'., Lallemand, P. Lattice BGK models for navier-stokes equation. Europhysics Letters. 1992. 17(6). Pp. 479–484.
17. Akai, T., Bijeljic, B., Blunt, M.J. Wetting boundary condition for the color-gradient lattice Boltzmann method: Validation with analytical and experimental data. Advances in Water Resources. 2018. Vol. 116. Pp. 56–66.
18. Chapman, S., Cowling, T.G. The mathematical theory of nonuniform gases: an account of the kinetic theory of viscosity, thermal conduction and diffusion in gases. 3rd ed. Cambridge: Cambridge University Press. 1970.
19. Stobiac, V., Tanguy, P.A., Bertrand, F. Boundary conditions for the lattice Boltzmann method in the case of viscous mixing flows. Computers & Fluids. 2013. Vol. 73. Pp. 145–161.
20. Chai, Z.H., Guo, Z.L., Shi, B.C. Prediction of permeability in porous media with multi-relaxation-time lattice Boltzmann method. Journal of Engineering Thermophysics. 2010. No. 1. Pp. 107–109. (Chinese)
21. Zhou, Q.S. Study on permeability of autoclaved aerated concrete block and the wall. Hangzhou: Zhejiang Sci-Tech University. 2018. (Chinese)
22. Korniyenko, S.V., Vatin, N.I., Gorshkow, A.S. Thermophysical field testing of residential buildings made of autoclaved aerated concrete blocks. Magazine of Civil Engineering. 2016. 64(4). Pp. 10–25. DOI: 10.5862/MCE.64.2
23. Fedosov, S.V., Rumyantseva, V.E., Krasilnikov, I.V., Konovalova, V.S., Evsyakov, A.S. Mathematical modeling of the colmatation of concrete pores during corrosion. Magazine of Civil Engineering. 2018. 83(7). Pp. 198–207. doi: 10.18720/MCE.83.18
24. Zhu, M.G., Wang, H., Liu, L.L., Ji, R., Wang, X.D. Preparation and characterization of permeable bricks from gangue and tailings. Construction and Building Materials. 2017. Vol. 148. Pp. 484–491.

Contacts:

Fu Jun, 13588717727; fujun@zstu.edu.cn
Yu Yue, +8617364522496; 2206105018@qq.com
Ye JiaBin, 15757124083; 1640092012@qq.com